UAV real-time location using a Wireless Sensor Network

J.-L. Rullán-Lara
Heudiasyc-UTC UMR CNRS 6599
Centre de Recherches de Royallieu
B.P. 20529 60205 Compiègne, France
Telephone: +33 (0)3 44 23 44 23
Email: jrullanl@hds.utc.fr

S. Salazar
LAFMIA UMI CNRS 3175
Av. Politécnico Nacional No. 2508
San Pedro Zacatenco, 07360
México, México
Email: sergio.salazar.cruz@gmail.com

R. Lozano
Heudiasyc-UTC UMR CNRS 6599
Centre de Recherches de Royallieu
B.P. 20529 60205 Compiègne, France
Telephone: +33 (0)3 44 23 44 23
Email: rlozano@hds.utc.fr

***Abstract*—A real-time localization algorithm is presented in this paper. The algorithm uses an Extended Kalman Filter and is based on time difference of arrivals (TDOA) measurements of radio signal. The position and velocity of an Unmanned Aerial Vehicle (UAV) are successfully estimated in closed-loop in real-time in both hover and path tracking flights. Relatively small position errors obtained from the experiments, proves a good performance of the proposed algorithm.**

I. Introduction

The position estimation (location) problem of an object is a research subject that has attracted a lot of interest during the recent years. Several applications on location of terrestrial and aerial robots, expensive computer equipment [1], [2], management of products and transportation [3], [4] and animals localization [5], [6] are reported in the literature. Unmanned aerial vehicles (UAV) is a major research area due to the large potential applications that such vehicles have in technological and industrial task. In addition, recent advances in electronics have dramatically improved the degree of integration of onboard control systems for UAVs.

For outdoor applications, GPS provides low errors in location estimation but they are significant for UAVs. In addition, it is not suitable for indoor applications or areas with dense foliage since this system uses satellites as beacons. Indeed, obstacles such as buildings, branches, leaves, etc, attenuate the GPS signals. Consequently, alternative strategies have to been proposed. A common issue is to use low cost ultrasonic or infrared sensors. This kind of sensor is limited to few meters and its accuracy depends on the brightness of the light and Line-of-sight (LOS) conditions in the environment.

Location systems based on the vision is another option that has also successfully been exploited. However, special cameras and a dedicated computer system to execute the image processing algorithms are required. In addition, image processing algorithms consume much of the computing resources. This is a significant disadvantage when dealing with real-time onboard applications where delays can affect the overall stability of the process.

Another approach is to measure some radio signal metrics such as RSS (received signal strenght), AOA (angle of arrival), TOA (time of arrival), and TDoA (time difference of arrival) by a set of wireless sensors around the source. *i.e.*, Wireless Sensor Networks (WSN). WSN can be used in both indoors and outdoors which gives them an advantage over GPS. More precisely, Chirp Spread Spectrum (CSS)-based communication protocol and chipset technology is shown to dominate the indoor localization market [7]. Symmetric double side two way ranging (SDS-TWR) is the key of CSS [7], [8] and consists in repeating the packet exchange twice, inverting the role of the two devices in the second exchange. SDS-TWR technology demonstrates a superiority over other localization methods in that it removes the time synchronization between devices, which is a quite demanding requirement and leading to an improved ranging accuracy. This type of WSN [9] is already used to find pallets and forklifts in warehouses [3], [4] but not in UAVs yet.

Noise is always present in radio signals and any other signal obtained from noisy radio signals, as distances derived from TDOA measurements, will be affected as well. Several mathematical methods have been developed based on different approaches [10], [11], [12]. The least squares (LS) and Kalman filter (KF) are widely employed for target positioning. By simulations in [13], the authors were proved a weighted least squares (CWLS) solution based on range measurements. Based on the Spherical Interpolation method [14], linear and quadratic constrained LS closed-forms solutions are derived in [16] and [17], respectively.

Kalman filter is a well-known and widely-used method to deal with noisy data and sensor fusion. In addition, internal states of a process not always directly accessible can be estimated. It is based on two main assumptions [18]: target motion and observation models are linear and, theirs errors and initial estimated probability distribution is Gaussian. The first assumption is not always true, however variants such as Extended Kalman Filter (EKF) [19] or Unscented Kalman Filter (UKF) [20] can be employed.

In this paper we offer to solve the localization problem for an UAV using SDS-TWR ranging [9]. The localization is based on Extended Kalman filter and is tested in real time.

The paper is organized as follows. In Section II we introduce the proposed localization algorithm and its application to an UAV. Experimental setup and results are described in Sections

III and IV, respectively. And the concluding remarks are finally given in Section V.

II. UAV LOCALIZATION

In this part, we develop the localization algorithm for an UAV. To simplify, we will consider the following assumptions:

1) The workspace of the flying robot is the xy plane defined by four bases stations.
2) The translational movements are given in manual mode.
3) An onboard attitude control stabilize the orientation of the UAV.
4) Linear motion at constant velocity are performed by the vehicle.

The position estimation is made through the Kalman filter. Some real-time applications using this technique and CSS ranging can be found in the literature. In [21], the position of a static wireless node was carried out with some significant improvements to compensate the offset in range measurements. Localization of forklift truck and pallets in warehouse were proposed in [3] and [22], respectively.

In the above cases, targets are quite different of UAV. An unmanned aerial vehicle is a unstable system with very fast dynamic which, even in hover flight, neither the condition static in [18] nor the dynamic of mobiles in [20] can not be considered at all. Then, the location should be sufficient to locate the UAV, at least, in an acceptable neighborhood of the real position.

A. Kalman Filter

The Kalman filter is an algorithm for efficient state estimation minimizing the covariance error [18], [23]. The basic filter is well-established, and it assumes that the transition and the observation models are linear. Due to nonlinearities in range measurements, Extended Kalman Filter must be applied. When the input is zero, the evolution of the state in time is given by a stochastic difference equations

$$\begin{aligned} \bar{\vartheta}_{k+1} &= \mathbf{f}(\bar{\vartheta}_k, \mathbf{w}_k) \\ \bar{\xi}_k &= \mathbf{h}(\bar{\vartheta}_k, \mathbf{v}_k) \end{aligned} \tag{1}$$

where $\bar{\vartheta}_k$ is the state vector at time k, $\bar{\xi}_k$ is the range vector process, and $\mathbf{f}(\cdot)$ and $\mathbf{h}(\cdot)$ are the nonlinear process and observation functions, respectively. The noise is represented by the vector $\mathbf{w}_k$ in the process and by vector $\mathbf{v}_k$ in the observation. Noises are assumed to be independent with gaussian distribution, that is, $\mathbf{w}_k \sim \mathcal{N}(0, \mathbf{Q})$ and $\mathbf{v}_k \sim \mathcal{N}(0, \mathbf{R})$. The initial state $\bar{\vartheta}_0$ is assumed to be normally distributed with mean ϑ_0 and covariance matrix $\mathbf{P}_0$.

The state and range functions are linearized as follows:

$$\mathbf{F}_k = \nabla_{\bar{\vartheta}} \mathbf{f}(\bar{\vartheta}_k)|_{\bar{\vartheta}_k = \hat{\bar{\vartheta}}_k}, \qquad \mathbf{H}_k = \nabla_{\bar{\vartheta}} \mathbf{h}(\bar{\vartheta}_k)|_{\bar{\vartheta}_k = \hat{\bar{\vartheta}}_k^-} \tag{2}$$

where $\hat{\bar{\vartheta}}_k$ and $\hat{\bar{\vartheta}}_k^-$ are the prior and the posterior mean estimates at time step k. Matrices $\mathbf{F}_k$ and $\mathbf{H}_k$ are the state transition matrix and the observation matrix, respectively. The system becomes

$$\begin{aligned} \bar{\vartheta}_{k+1} &= \mathbf{F}_k \bar{\vartheta}_k + \mathbf{w}_k \\ \bar{\xi}_k &= \mathbf{H}_k \bar{\vartheta}_k + \mathbf{v}_k \end{aligned} \tag{3}$$

The time and measurement update for the EKF are

$$\begin{cases} \hat{\bar{\vartheta}}_{k+1|k} &= \mathbf{f}_k(\hat{\bar{\vartheta}}_{k|k}, 0) \\ \mathbf{P}_{k+1|k} &= \mathbf{F}_k \mathbf{P}_{k|k} \mathbf{F}_k^T + \mathbf{Q}_k. \end{cases} \tag{4}$$

$$\begin{cases} \hat{\bar{\vartheta}}_{k|k} &= \hat{\bar{\vartheta}}_{k+1|k} + \mathbf{K}_k \bar{\nu}_k \\ \bar{\nu}_k &= \bar{\xi}_k - \mathbf{h}_k(\hat{\bar{\vartheta}}_{k+1|k,0}) \\ \mathbf{K}_k &= \mathbf{P}_{k+1|k} \mathbf{H}_k^T \mathbf{S}_k^{-1} \\ \mathbf{S}_k &= \mathbf{H}_k \mathbf{P}_{k+1|k} \mathbf{H}_k^T + \mathbf{R}_k \\ \mathbf{P}_{k|k} &= (\mathbf{I} - \mathbf{K}_k \mathbf{H}_k) \mathbf{P}_{k+1|k} \end{cases} \tag{5}$$

where $\mathbf{P}_k$ is error prediction covariance matrix, $\bar{\nu}_k$ is the innovation and $\mathbf{S}_k$ is its covariance matrix and $\mathbf{K}_k$ is the filter gain.

B. Localization

Under assumptions, the localization problem reduces to estimate the position and velocity of the aircraft in a plane, then a continuous white noise acceleration model can be considered. Consequently, the state transfer matrix, $\mathbf{F}_k$, yields a 4×4 constant matrix

$$\mathbf{F}_k = \begin{pmatrix} 1 & 0 & \Delta & 0 \\ 0 & 1 & 0 & \Delta \\ 0 & 0 & 1 & 0 \\ 0 & 0 & 0 & 1 \end{pmatrix} \tag{6}$$

where Δ is the constant sampling period of the TDOA measurements. Therefore, the state vector, $\bar{\vartheta}_k$, only contains the UAV position and velocity components, *i.e.*

$$\bar{\vartheta}_k = \begin{pmatrix} x_k & y_k & \dot{x}_k & \dot{y}_k \end{pmatrix}^T. \tag{7}$$

Let $\mathbf{x_i} = (x_i, y_i)^T$ be the known position of the ith base station (BS_i). The distance d_i between the UAV and the BS_i, is given by

$$\begin{aligned} d_k^i &= \|\bar{\vartheta}_k^p - \mathbf{x}_i\| \\ &= \sqrt{(x_k - x_i)^2 + (y_k - y_i)^2}, \quad i = 1, 2, \ldots, N \end{aligned} \tag{8}$$

where $\bar{\vartheta}_k^p$ is related to $\bar{\vartheta}_k$ through

$$\bar{\vartheta}_k^p = \begin{pmatrix} x_k & y_k \end{pmatrix}^T. \tag{9}$$

From (8), note that the observed process is not linear and the function $\bar{\xi}_k = \mathbf{h}(\bar{\vartheta}_k)$, in our case $N = 4$, becomes

$$\bar{\xi}_k = \begin{pmatrix} \|\bar{\vartheta}_k^p - \mathbf{x}_1\| \\ \|\bar{\vartheta}_k^p - \mathbf{x}_2\| \\ \|\bar{\vartheta}_k^p - \mathbf{x}_3\| \\ \|\bar{\vartheta}_k^p - \mathbf{x}_4\| \end{pmatrix} \tag{10}$$

Thus, the observation matrix $\mathbf{H}_k$ for (10) is

$$\mathbf{H}_k = \begin{pmatrix} \frac{x_k - x_1}{\|\bar{\vartheta}_k^p - \mathbf{x}_1\|} & \frac{y_k - y_1}{\|\bar{\vartheta}_k^p - \mathbf{x}_1\|} & 0 & 0 \\ \frac{x_k - x_2}{\|\bar{\vartheta}_k^p - \mathbf{x}_2\|} & \frac{y_k - y_2}{\|\bar{\vartheta}_k^p - \mathbf{x}_2\|} & 0 & 0 \\ \frac{x_k - x_3}{\|\bar{\vartheta}_k^p - \mathbf{x}_3\|} & \frac{y_k - y_3}{\|\bar{\vartheta}_k^p - \mathbf{x}_3\|} & 0 & 0 \\ \frac{x_k - x_4}{\|\bar{\vartheta}_k^p - \mathbf{x}_4\|} & \frac{y_k - y_4}{\|\bar{\vartheta}_k^p - \mathbf{x}_4\|} & 0 & 0 \end{pmatrix} \tag{11}$$

Notice that all elements of (11) have singularities if $\|\bar{\vartheta}_k^p - \mathbf{x}_i\| = 0$, $i = 1, 2, 3, 4$.

III. Experimental set up

A. Quad-rotor vehicle

The flying robot is the classical quad-rotor which is mechanically simpler than a classical helicopter since it does not have a swashplate and have constant pitch blades, see Fig. 1. It has two counter rotating pairs of propellers arranged in a square. In the middle of the square, the onboard computer, the inertial measurement unit (IMU), the location sensor board, and the batteries are mounted.

The thrust is provided by four Robbe Roxxy BL-Motor 2827-34 brushless motors and four YGE30i speed controllers. A homemade IMU is used to compute the attitude angles. The roll (ϕ), pitch (θ), and yaw (ψ) angles are estimated by using three-axis accelerometer (ADXL203) and a compass module (CMPS03). The angular rates, $\dot{\phi}$ and $\dot{\theta}$, are measured by an integrated dual-axis gyroscope (IDG-500) and the yaw angle rate, $\dot{\psi}$, is measured by a single yaw rate gyroscope (ADXRS613). The altitude is determined using an ultrasonic sensor (SPF03).

The onboard hardware is based on a RCM3400 analog RabbitCore which runs at 29.4 MHz. An I2c protocol control signal is sent to the speed controllers every sampling period. The attitude dynamic, $\ddot{\eta} = \tau$, $\eta : \phi, \theta, \psi$, is stabilized onboard using the following control input based the integrators in cascade with bounded input as in [24]

$$\tau = -\sigma_1(k_1\dot{\eta}) - \sigma_2(k_2\eta) \tag{12}$$

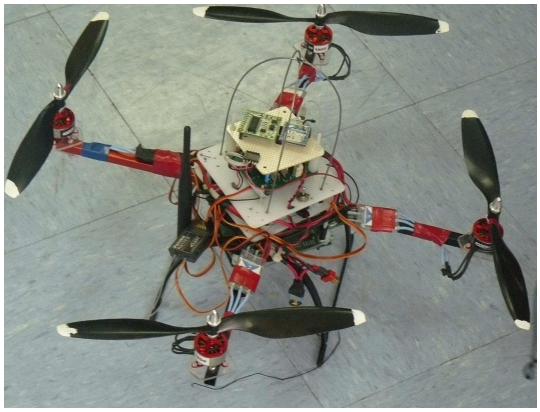

Fig. 1. Quad-rotor UAV

B. Distance measurement system

The NanoLOC development kit from Nanotron Technologies has been used to measure the distances between the BS. Nanotron Technologies has developed a Wireless Sensor Network (WSN) which can work as a Real-Time Location Systems (RTLS) [7]. The distance between two wireless nodes is determined by their Symmetrical Double-Sided Two Way Ranging (SDS-TWR) technique, which allows a distance measurement by means of the signal propagation delay. It estimates the distance between two nodes by measuring the TDOA symmetrically from both sides.

Wireless communications as well as the ranging methodology SDS-TWR are integrated in a single chip, the nanoLOC TRX Transceiver [7]. The transceiver operates in the ISM band of 2.4 GHz and supports location-aware applications including Location Based Services (LBS) and asset tracking applications. The wireless communication is based on Nanotron's patented modulation technique Chirp Spread Spectrum (CSS) according to the wireless draft standard IEEE 802.15.4a. [25].

SDS-TWR measures the round trip time between two node, A and B, and avoids the need to synchronize the clocks. To avoid the drawback of clock drift the range measurement is preformed twice and symmetrically and is obtained using the following formula [9]

$$D_{AB} = \frac{(T_1 - T_2) + (T_3 - T_4)}{4} \tag{13}$$

where T_1 is the propagation delay time of a round trip between Node A and Node B, T_2 is the processing delay in Node B, T_3 is the propagation delay time of a round trip between Node B and Node A and T_4 is the processing delay in Node A.

The NanoLOC development kit contains five sensor boards with sleeve dipole omnidirectional antennas. One target board, *TAG* board, is mounted in the UAV and the base station boards are placed in rectangular geometry (see Fig. 4).

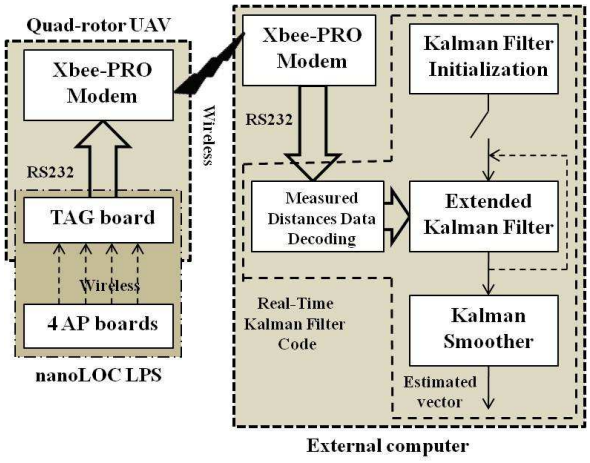

Fig. 2. Kalman filter implementation block diagram

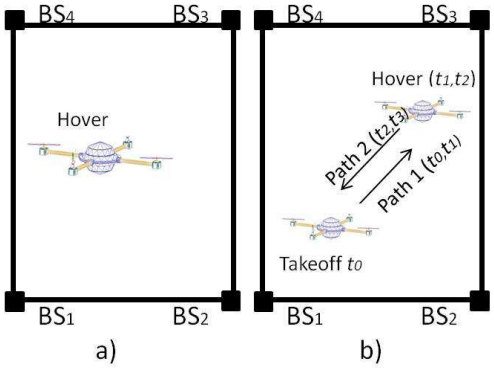

Fig. 3. Experimental set up

To measure the real distances between the helicopter and the base stations, a wireless link is added. This link is made by using two XBee-PRO modem whose communicate the helicopter and an external computer where the algorithm is executed in real time. Figure 2 shows the real-time closed loop localization algorithm scheme. Target board and the BS boards exchange data. Then, TAG board sends a codified message with the measured distances by serial communication link to a XBee-PRO modem. This last message is sent immediately to the external computer. A frame data of 68 bytes is decoded to find out the four actual measured distances values d_k^1, d_k^2, d_k^3, and d_k^4. Finally, the innovation $\bar{\nu}_k = \bar{\xi}_k - \hat{\bar{\xi}}_k$, is computed as follows:

$$\bar{\nu}_k = \begin{pmatrix} d_k^1 \\ d_k^2 \\ d_k^3 \\ d_k^4 \end{pmatrix} - \begin{pmatrix} \|\hat{\vartheta}_k^p - \mathbf{x}_1\| \\ \|\hat{\vartheta}_k^p - \mathbf{x}_2\| \\ \|\hat{\vartheta}_k^p - \mathbf{x}_3\| \\ \|\hat{\vartheta}_k^p - \mathbf{x}_4\| \end{pmatrix} \tag{14}$$

The prediction and the update steps of the localization algorithm are performed at $\Delta = 100$ms. Once these tasks ($\hat{\vartheta}_{k|k-1}$, $\hat{\vartheta}_{k+1|k+1}$, $\mathbf{P}_{k|k-1}$, $\mathbf{P}_{k+1|k+1}$) have been completed, one-step Kalman smoother is executed to obtain $\hat{\vartheta}_{k|k+1}$ and $\mathbf{P}_{k|k+1}$, see Fig. 2.

IV. Experimental results

Experiments have been carried out indoor with the UAV flying in manual mode. Sets of data were collected on several times (during 40 seconds) to verify the correct functioning of the proposed localization algorithm in closed-loop. The measurement noise is considered as Gaussian noise $w_{i,k} \sim \mathcal{N}(0, \sigma_i)$ and σ_i is obtained by experiments. The final values of covariance matrices are $\mathbf{R} = 0.45\mathbf{I}$ and $\mathbf{Q} = 10 \times 10^{-5}\mathbf{I}$.

The performance of the proposed algorithm was tested in two kind of experiments. First, the UAV is flying in hover while the second test is devoted to evaluate the path tracking accuracy of the algorithm. These experiments are illustrated in Fig. 3.

A. Hover flight test

The workspace of the UAV is delimited by the BSs placed in the positions $BS_1 = (0, 0)$, $BS_2 = (0, 4.5\text{m})$, $BS_3 = (4.5\text{m}, 4\text{m})$ and $BS_4 = (0, 4\text{m})$, see Fig. 4. The experiment consist in hover flight of the UAV over the point $(1.75\text{m}, 2\text{m})$.

Figure 4 shows the estimated position when the algorithm is applied in real-time. Note that the UAV estimated position remains around the desired point during all experiment. The estimated position values are $\hat{x} = 1.52$m and $\hat{y} = 2.20$m with standard deviations of $\sigma_{\hat{x}} = 0.1374$m and $\sigma_{\hat{y}} = 0.1224$m, respectively.

Another way to evaluate the performance of the proposed algorithm is through confidence intervals showed in Fig 5. From this graph, observe that the estimated position remains within the confidence interval, *i.e.*, 90% of data are in around the mean value and very few values are beyond this range. Therefore, we conclude that the proposed location algorithm correctly estimates the position of the UAV in hover, with a relatively small error.

Remember that the helicopter is in hovering, and from Fig. 6 note that the estimated speeds is close to zero, which is according to this condition. The pick values ($\sim 1m/s$) follow from the small corrections given by the pilot.

B. Path tracking flight test

In order to allow sufficient movement for the UAV, a larger workspace is used. For this case, the base stations were place at points $BS_1 = (0, 0)$, $BS_2 = (0, 8.5\text{m})$, $BS_3 = (8.5\text{m}, 6\text{m})$ and $BS_4 = (0, 6\text{m})$.

Three parts are included in this experiment, see Fig. 7. The first and third parts are devoted to trajectory tracking whereas the second one is dedicated to hover flight. Thus, from t_0 to t_1 the pilot moves the UAV following a straight line from point $(1.75\text{m}, 2\text{m})$ to point $(6\text{m}, 5\text{m})$. From Fig. 7, note that both $\hat{x}$ and $\hat{y}$ are a little far from the desired path. This comes from the fact that when the UAV is launched the

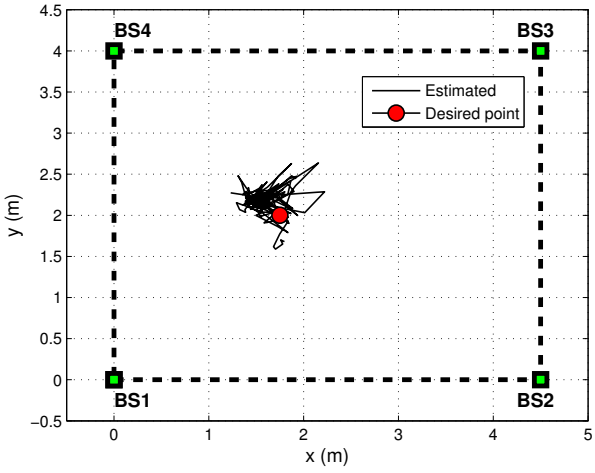

Fig. 4. Estimated position in hover flight

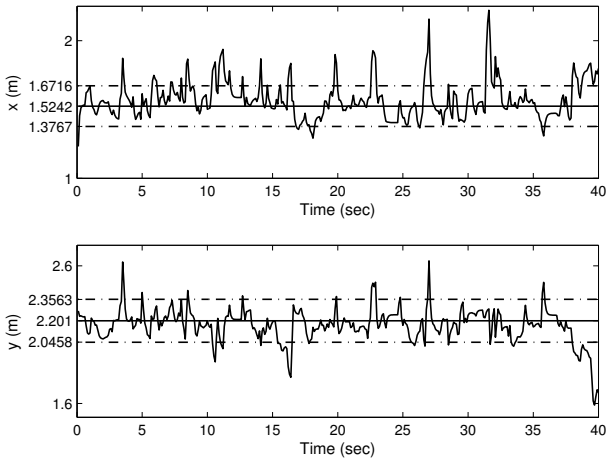

Fig. 5. Variances of $\hat{x}$ and $\hat{y}$ in hover flight

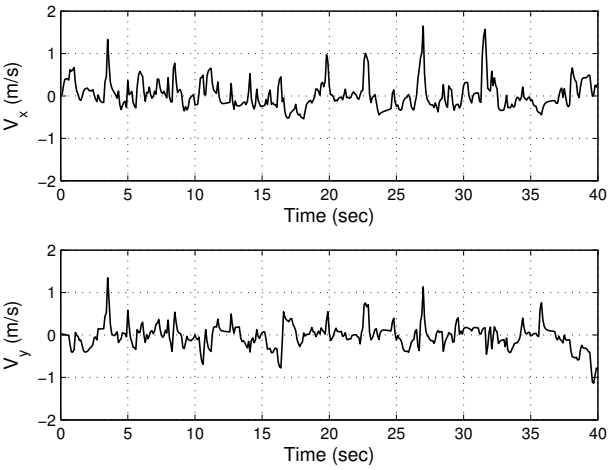

Fig. 6. Estimated velocities in hover flight

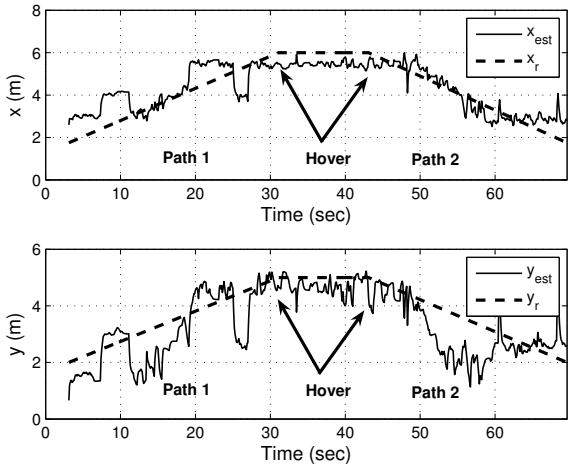

Fig. 7. Estimated $\hat{x}$ and $\hat{y}$ in path following

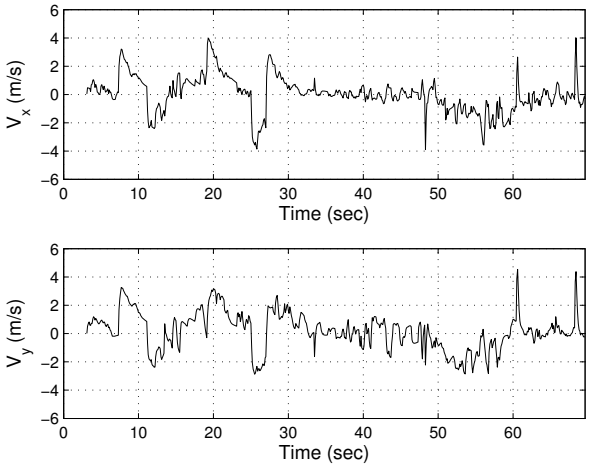

Fig. 8. Estimated velocity in path following

pilot tried to bring the UAV along the path. This fact can also be observed in the estimated speeds shown in Fig 8. The velocities magnitudes are great at the beginning which expresses abrupt linear movements of the vehicle, given by the pilot.

From t_1 to t_2, Fig. 7, the helicopter is in hover flight over the point $(6\mathrm{m}, 5\mathrm{m})$. We note that during this period, the best estimation is obtained. Finally, from t_2 to t_3 the helicopter returns to the starting point. From Figs. 7-8 we can conclude that for tracking, and obviously for hover, the results are satisfactory.

V. Conclusions

Real-time estimation of position and velocity of an UAV have been presented in this paper by using the time difference of arrival method applied to a local positioning system (LPS). The LPS is composed of five transceiver cards which exchange information between them.

The obtained TDOA measurements model is nonlinear and an Extended Kalman Filter were applied in order to estimate the states. The proposed localization algorithm has been successfully tested in closed-loop in real-time experiments for hover flight and for path following. The best results were found in hover test and this performance is related to the form of the transfer matrix $\mathbf{F}_k$. However, with quasi-constant displacement, the algorithm continues making a good estimation of position. Finally, the experimental results have proved the well performance of the proposed algorithm with small estimation errors.

Current research work is focused on including the proposed localization algorithm into the stabilization control loop of the UAV. We work to carry out autonomous navigation experiments with an UAV.

ACKNOWLEDGMENTS

The first author thanks the Universidad Autónoma del Carmen (UNACAR) and the Secretaría de Educación Pública (SEP) for their financial support PROMEP/103.5/07/2057. He also tanks to Dr. P. Castillo, a researcher of Heudiasyc Laboratory, the comments and corrections during the development of this paper.

REFERENCES

[1] J. Yim, C. Park, J. Joo, S. Jeong, Extended Kalman Filter to wireless LAN based indoor psoitioning, Decision Support Systems, Elsevier, Vol. 45, pp. 960-971, 2008.

[2] J. Yim, S. Jeong, K. Gwon, J. Joo, Improvement of Kalman filters for WLAN based indoor tracking, Expert Systems with Applications, Elsevier, Vol. 37, Issue 1, pp. 426-433, 2010.

[3] C. Röhrig and S. Spieker, Tracking of Transport Vehicles for Warehouse Management using a Wireless Sensor Network, 2008 IEEE/RSJ International Conference on Intelligent Robots and Systems, Nice, France, Sept, 22-26, 2008.

[4] C. Röhrig, M. Muller, Localization of Sensor Nodes in a Wireless Sensor Network Using the nanoLOC TRX Transceiver, IEEE 69th Vehicular Technology Conference Spring, 26-29 April 2009 Barcelona, Spain.

[5] P. Soriano, F. Caballero y A. Ollero. RF-based Particle Filter localization for Wildlife Tracking by using an UAV. 40 th International Symposium of Robotics. Marzo 2009. Barcelona, España.

[6] F. A Togersen, F. Skjoth, L. Munksgaard, S. Hojsgaard, Wireless indoor tracking network based on Kalman filters with an applications to monitoring dairy cows, Computer and Electronics in Agriculture, Elsevier, Vol. 72, pp. 119-126, 2010.

[7] Nanotron Technologies GmbH, "Real Time Localization Systems (RTLS)", White paper, 2006

[8] H.-S. Ahn, H. Hur, W.-S. Choi, One-way Ranging Technique for CSS-based Indoor Localization, IEEE International Conference on Industrial Informatics, Daejeon, Korea, 2008.

[9] Nanotron Technologies GmbH, "nanoLOC Development Kit User Guide", Technical Report NA-06-0230-0402-2.0, 2008

[10] D.J. Torrieri, Statistical Theory of Passive Location Systems, IEEE Transaction on Aerospace and Electronic Systems, Vol. AES-20 Issue 2, pp. 183-198, March 1984.

[11] G. Mao, B. Fidan, B. D. O. Anderson, Wireless sensor network localization techniques, Computer Networks, Vol. 51, Issue 10, pp. 2529-2553, 11 July 2007.

[12] F. Seco, A. Jiménez, C. Prieto, J. Roa, and K. Koutsou, A survey of Mathematical Methods for Indoor Localization, IEEE 6th International Symposium on Intelligent Signal Processing, 26-28 August, 2009, Budapest, Hungry.

[13] K. Dogancaya, , A. Hashemi-Sakhtsari, Target tracking by time difference of arrival using recursive smoothing, Signal Processing 85 (2005) 667–679.

[14] J. O. Smith and J. S. Abel, Closed-form least-squares location estimation from range-difference measurements, *IEEE Trans. Acoust. Speech, Signal Processing*, vol. ASSP-35, pp 1661-1669, Dec. 1987.

[15] Y.T.Chan and K.C.Ho, A simple and efficient estimator for hyperbolic location, IEEE Transaction on Signal processing, August, 1994.

[16] Y. Huang, J. Benesty, G. W. Elko, and R. M. Mersereati, Real-time Passive Source Localization: A Practical Linear-Correction Least-Squares Approach, *IEEE Transactions on Speech and Audio Processing*, vol. 9, no. 8, pp 943-956, 2001.

[17] K. W. Cheung, H. C. So, W.-K. Ma, Y. T. Chan, A Constrained Least Squares Approach to Mobile Positioning: Algorithms and Optimality, EURASIP Journal on Applied Signal Processing, Vol. 2006, Article ID 20858, pp. 1-23, 2006.

[18] R.E. Kalman, "A new approach to linear filtering prediction problems", ASME Journal of Basic Engineering, Vol. 82, pp. 34-45, 1960.

[19] V. M. Becerra, P. D. Roberts, G. W. Griffiths, Appliyingthe extended Kalman filter to systems described by nonlinear differential-algebraic equations, *Control Engineering Practice*, Volume 9, Issue 3, March 2001, pp 267-281.

[20] S. J. Julier, J. K. Ulhmann, A new extension of the Kalman filter to nonlinear systems, in Proceedings of the American Control Conference, 1995, pp. 1628-163.

[21] H. Cho, C. W. Lee, S. J. Ban S. W. Kim, An enhanced positioning scheme for chirp spread spectrum ranging, *Expert Systems with Applications*, Volume 37, Issue 8, August 2010, pp 5728-5735.

[22] C. Röhrig and S. Spieker, Localization of Pallets in Warehouses using Wireless Sensor Networks, 16th Mediterranean Conference on Control and Automation, 2008, pp 1833-1838.

[23] Y. Bar-Shalom, X.-Rong Li, T. Kirubarajan, Estimation with Applications to Tracking and Navigation, John Wiley Sons, Inc. New York, 2001.

[24] G. Sanahuja, P. Castillo, A. Sanchez, Stabilization of n integrators in cascade with bounded input with experimental application to a VTOL laboratory system, *International Journal of Robust and Nonlinear Control*, Vol. 20, Issue 10, pp 1129-1139, 10 July 2010, DOI: 10.1002/rnc.1494.

[25] L. De Nardis, M.-G. Di Benedetto, Overview of the IEEE 802.15.4/4a standards for low data rate Wireless Personal Data Networks, 4th Workshop on Positioning, Navigation and Communication, Hannover, Germany, 2007.